Theoretical modeling of exciton-light coupling in quantum wells

2016 J. Phys.: Conf. Ser. 690 012018

(http://iopscience.iop.org/1742-6596/690/1/012018)

Journal of Physics: Conference Series **690** (2016) 012018 doi:10.1088/1742-6596/690/1/012018

Theoretical modeling of exciton-light coupling in quantum wells

E S Khramtsov[1], P A Belov[2], P S Grigoryev[1], I V Ignatiev[1], S Yu Verbin[1] and S L Yakovlev[2]

[1]Spin Optics Laboratory, St. Petersburg State University, 7/9 Universitetskaya nab., St. Petersburg, 199034 Russia
[2]Department of Physics, St. Petersburg State University, 7/9 Universitetskaya nab., St. Petersburg, 199034 Russia

E-mail: e.khramtsov@spbu.ru

Abstract. The wave function of excitons in GaAs-based finite square quantum wells (QWs) is calculated by the direct numerical solution of the three-dimensional Schrödinger equation. The precise results for the lowest exciton state are obtained by the Hamiltonian discretization using the fourth-order finite-difference scheme. The radiative decay rate is calculated for QWs of various widths using the obtained exciton wave function.

1. Introduction

The theoretical modeling of excitons in a bulk semiconductor is usually carried out in the framework of the hydrogen model [1]. This model, however, becomes unsuitable for semiconductors with a degenerate valence band. In such a case, the exciton Hamiltonian should be generalized by introduction of the Luttinger terms describing the complex valence band [2]. The terms couple the exciton center-of-mass and intrinsic electron-hole motions. As a result, the variables of the exciton Schrödinger equation (SE) cannot be separated and one has to consider the multi-dimensional SE [3]. A study of the exciton in a quantum well (QW) meets further complications of the problem. Even in the simplest case, when only the diagonal part of the Luttinger Hamiltonian is included into the problem, the presence of the QW potential requires one to consider at least the three-dimensional SE, which cannot be solved analytically.

The calculations of the exciton radiative decay rate (or the oscillator strength) have been carried out in several works using different simplifications of the problem [4-8] The experimental studies of the radiative characteristics are widespread, see, e.g., Refs. [9-14] Recent measurements of the radiative decay rate have been carried out by Poltavtsev *et al.* [15, 16]. These experimental results and lack of the available theoretical calculations motivated us for this study.

In the present paper, we report on the results of calculations of the radiative decay rate for QWs of various widths. The radiative decay rate is obtained using the wave function found from the SE for excitons in QWs with a degenerate valence band. Partial separation (over two variables) of the center-of-mass motion and cylindrical symmetry of the problem allowed us to reduce the initial SE to the three-dimensional one. The numerical solution of the problem has been done for the GaAs/AlGaAs and InGaAs/GaAs QWs, which are widely experimentally and theoretically studied now as model heterostructures [13, 17].

2. Microscopic model

In our study, we assume that the exciton in a QW is described by the SE with the diagonal part of the Luttinger Hamiltonian [2] only:

$$H = \frac{\mathbf{k}_e^2}{2m_e} + \frac{\left(k_{hx}^2 + k_{hy}^2\right)}{2m_{hxy}} + \frac{k_{hz}^2}{2m_{hz}} - \frac{e^2}{\epsilon|\mathbf{r_e} - \mathbf{r_h}|} + V_e(\mathbf{r_e}) + V_h(\mathbf{r_h}). \tag{1}$$

Here, indices e and h denote the electron and the hole, respectively. The relative electron-hole distance is $|\mathbf{r_e} - \mathbf{r_h}|$. The electron charge is denoted by e and the dielectric constant is ϵ. The square QW potentials $V_e(\mathbf{r_e})$ and $V_h(\mathbf{r_h})$ are zero inside the QW and equal to some constant values in the barriers (conduction- and valence-band offsets, respectively). Term $\mathbf{k}_e^2/2m_e$ is the kinetic operator of the electron in the conduction band in the effective-mass approximation [3]. The kinetic terms of the hole in the valence band, the second and third terms in Eq. (1), come from the diagonal part of the Luttinger Hamiltonian [2].

Hamiltonian (1) specifies the six-dimensional SE, $H\Psi = E\Psi$, for the electron and the hole in QW coupled by the Coulomb interaction. The translational symmetry along the QW layer allows us to reduce this equation to the four-dimensional one by separation of the center-of-mass motion in the (x, y)-plane. This motion is described by an analytical part of the complete wave function, Ψ. The relative motion of the electron and the hole in the exciton is described by $\psi(x, y, z_e, z_h)$, where $x = x_h - x_e$, $y = y_h - y_e$. One more dimension is eliminated by taking advantage of the cylindrical symmetry of the problem and introducing the polar coordinates (ρ, ϕ) for description of the relative motion, since the Coulomb potential does not depend on ϕ. Representing the wave function in the form

$$\psi(x, y, z_e, z_h) = \psi(z_e, z_h, \rho)e^{ik_\phi\phi} = \frac{\chi(z_e, z_h, \rho)}{\rho}e^{ik_\phi\phi}, \tag{2}$$

where $k_\phi = 0, 1, 2, \ldots$, we proceed to the three-dimensional equation, which is numerically studied in the present paper. In Eq. (2), we introduce a factor $1/\rho$ in order to fulfill the cusp condition at $\rho = 0$.

Since the light interacts mainly with the ground $1s$ state of the exciton, we study the case when $k_\phi = 0$. In this case, the equation under consideration is written as [18]:

$$\left(K - \frac{e^2}{\epsilon\sqrt{\rho^2 + (z_e - z_h)^2}} + V_e(z_e) + V_h(z_h)\right)\chi(z_e, z_h, \rho) = E_x\chi(z_e, z_h, \rho) \tag{3}$$

where the kinetic term reads:

$$K = -\frac{\hbar^2}{2m_e}\frac{\partial^2}{\partial z_e^2} - \frac{\hbar^2}{2m_{hz}}\frac{\partial^2}{\partial z_h^2} - \frac{\hbar^2}{2\mu}\left(\frac{\partial^2}{\partial\rho^2} - \frac{1}{\rho}\frac{\partial}{\partial\rho} + \frac{1}{\rho^2}\right), \tag{4}$$

and $\mu = m_e m_{hxy}/\left(m_e + m_{hxy}\right)$ is the reduced exciton mass in the (x, y)-plane. The obtained three-dimensional Eq. (3) cannot be solved analytically because the potential terms do not allow further separation of the variables.

3. Numerical method

We performed the direct numerical solution of Eq. (3) for precise calculations of the exciton ground state energy, E_x, and function $\chi(z_e, z_h, \rho)$. The exponential decrease of the exciton wave function at large values of variables allows us to impose the zero boundary conditions at the boundary of some rectangular domain. The size of this domain varies from dozens of

QW widths (for small widths) down to several QW widths (for large widths). Therefore, the studied boundary value problem (BVP) is formed by Eq. (3) and the zero boundary conditions at $\rho = 0$, at some large value of ρ, and at large positive and negative values of variables $z_{e,h}$. The direct numerical solution of the BVP is feasible using available computational facilities. For this purpose, we employed the fourth-order finite-difference (FD) approximation [19] of the derivatives in Eq. (3) on the equidistant grids over three variables. We use the central fourth-order FD formula for approximation of the second partial derivative of $\chi(z_e, z_h, \rho)$ with respect to z_e:

$$\frac{-\chi_{k-2,l,m} + 16\chi_{k-1,l,m} - 30\chi_{k,l,m} + 16\chi_{k+1,l,m} - \chi_{k+2,l,m}}{12\Delta_{z_e}^2}. \tag{5}$$

Here, the unknown function on the grid, $\chi(z_{e,k}, z_{h,l}, \rho_m)$, is denoted as $\chi_{k,l,m}$. The same FD formula is employed for the second derivative with respect to z_h. We apply the noncentral fourth-order FD formulas for approximation of the first and second partial derivatives of $\chi(z_e, z_h, \rho)$ with respect to ρ. In the calculations, the grid steps over each variable have been taken to be the same, Δ.

Formula (5) defines the theoretical uncertainty of the numerical solution of the order of Δ^4 as $\Delta \to 0$. However, the discontinuity of the square potential at the QW interfaces decreases the convergence rate of the solution over z_e and z_h to order of Δ^2, whereas the convergence rate over variable ρ is kept $\sim \Delta^4$. The precise values of the studied quantities are obtained by the extrapolation of the results of calculations as the grid step goes to zero.

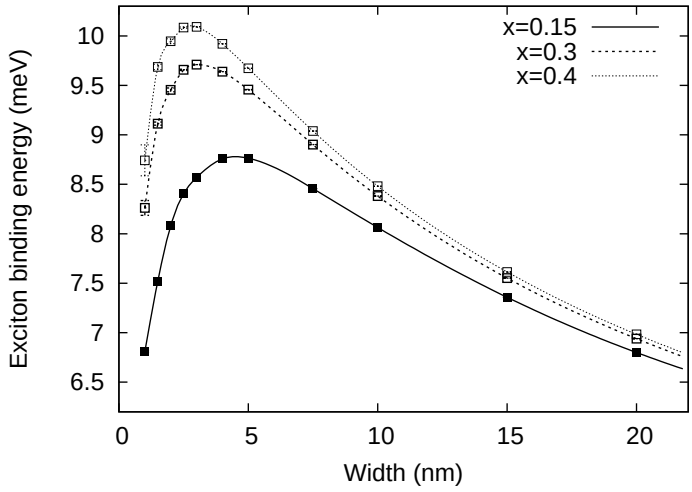

Figure 1. The calculated exciton binding energy for $GaAs/Al_xGa_{1-x}As$ for various aluminium concentrations: $x = 0.15, 0.3, 0.4$.

The nonzero solution of homogeneous equation (3) with trivial boundary conditions can be obtained by the diagonalization of the matrix constructed from the operator of this equation. This square matrix is large, non symmetric and sparse. The typical size of the matrix is of the order of 10^6, so that we keep in the calculations only nontrivial matrix elements of a few diagonals. The full diagonalization of such a matrix is impossible. However, a small part of the spectrum can be easily obtained using the Arnoldi algorithm [20]. As a result, we have calculated the lowest eigenvalue of the matrix and the corresponding eigenfunction. Thus, the ground state energy, E_x, and the corresponding wave function have been obtained for various widths of QW.

We applied the numerical algorithm for solving the SE with parameters for the $GaAs/Al_xGa_{1-x}As$ and $In_xGa_{1-x}As/GaAs$ QWs. The material parameters used for solving the eigenvalue problem (3) are based on the data from Ref. [21] for AlGaAs and from Ref. [8, 22] for InGaAs. In particular, the ratios of potential barriers were taken to be $V_e/V_h = 65/35$. The

difference of the electron and hole masses in the QW and in the barrier layers as well as the discontinuity of the dielectric constant at the QW interfaces were ignored.

To check the accuracy of the numerical procedure, we have calculated the exciton binding energy, R_x, which is defined with respect to the quantum confinement energy of the electron, E_e, and the hole, E_h, in QW by the formula $R_x = E_e + E_h - E_x$. Energies E_e and E_h are obtained from the solution of the corresponding one-dimensional SEs for the electron and the hole in QW. The results are shown in Figure 1 for the $GaAs/Al_xGa_{1-x}As$ QW with three barrier heights governed by the aluminium content. The results obtained agree well with other results reported, e.g., in Refs. [18, 21]. We should note here that the usual approach based on the effective mass approximation used in our work may give rise to inaccurate results for very thin (< 10 monolayers) QWs, where one monolayer is ≈ 0.28 nm for GaAs. In the thin QWs, the band mixing at the interfaces becomes important. The interface short-range corrections for this approach can be used in this case to obtain more accurate results [23].

4. Exciton-light coupling

The radiative properties of an exciton are defined by the parameter, called the radiative decay rate or the oscillator strength, see Refs. [1, 4, 5, 24]. The radiative decay rate, Γ_0, characterizes the decay of electromagnetic field emitted by the exciton ensemble after the pulsed excitation: $E(t) = E(0)\exp(-\Gamma_0 t)$. A consistent exciton-light coupling theory is presented in the monograph of Ivchenko [24]. It gives the expression for Γ_0:

$$\Gamma_0 = \frac{2\pi q}{\hbar\epsilon}\left(\frac{e|p_{cv}|}{m_0\omega_0}\right)^2 \left|\int_{-\infty}^{\infty} \Phi(z)\exp(iqz)dz\right|^2, \tag{6}$$

where $q = \sqrt{\epsilon}\omega/c$ is the light wave vector, ω_0 is the exciton frequency, $|p_{cv}| = \langle u_v|\epsilon\cdot\mathbf{p}|u_c\rangle$

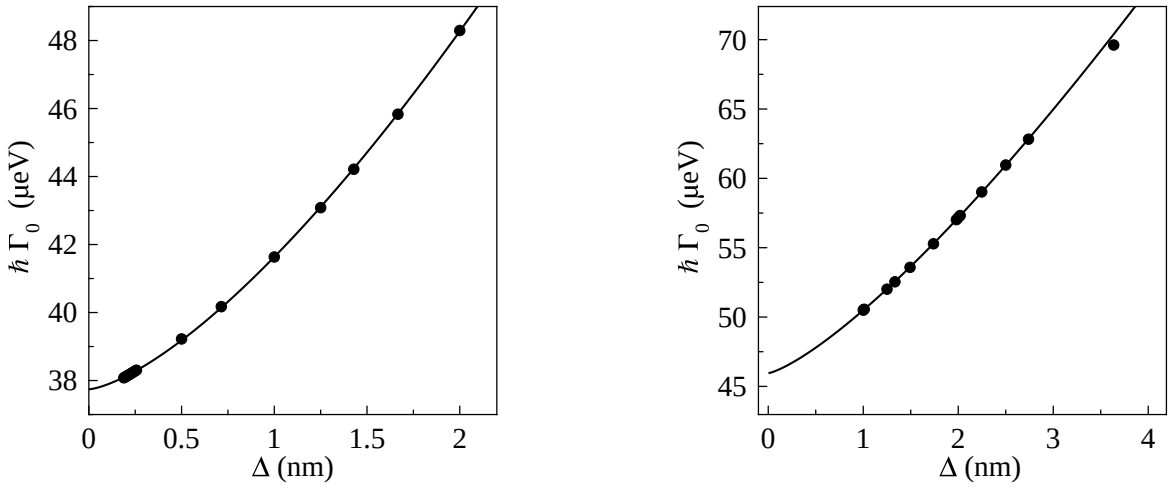

Figure 2. The dependence of the radiative decay rate, $\hbar\Gamma_0$, on the grid step, Δ, for QW width $L = 10$ nm (left panel) and for QW width $L = 200$ nm (right panel). The solid points are the values of the radiative decay rate calculated using the fourth-order FD scheme. The solid line indicates the fit of the calculated values by function $y = a\Delta^b + c$.

is the matrix element of the momentum operator between the single-electron conduction- and valence-band states, and $\Phi(z) \equiv \psi(z, z, 0)$ that is when $z = z_e = z_h$ and $\rho = 0$. The wave

function obtained from the microscopic calculation allowed us to calculate the radiative decay rate Γ_0 of the exciton ground state according to Eq. (6). The convergence of $\hbar\Gamma_0$ as the grid step Δ goes to zero is shown in Figure 2. The precise results are obtained by the extrapolation of Δ to 0.

We calculated Γ_0 for GaAs/$Al_{0.3}Ga_{0.7}$As and $In_{0.02}Ga_{0.98}$As/GaAs QWs of various widths in the ranges of $1 \div 300$ nm and $1 \div 200$ nm, respectively. In calculations, $|p_{cv}|^2 = m_0 E_p/2$, where $E_p = 28.8$ eV for GaAs and $E_p = 21.5$ eV for InAs are taken from Ref. [22]. The exciton frequency ω_0 is calculated using bandgap $E_g = 1.520$ eV for GaAs [24] and relevant parameters from [21, 22].

Figure 3 shows the radiative decay rate in energy units, $\hbar\Gamma_0$, as a function of the QW width. The radiative decay rate reaches its maximum at the QW width of about 130 nm. It approximately corresponds to the half of the light wavelength in the QW material. So, this maximum of Γ_0 corresponds to the maximal overlap of the exciton wave function $\Phi(z)$ and the light wave, see Eq. (6). For thick QWs, $L > 150$ nm, the calculated decay rate decreases with the well width rise, which can be qualitatively explained by the decrease of the overlap. The applicability of our model for the GaAs/AlGaAs QWs, however, may be limited. The energy distance between the heavy-hole and light-hole exciton states becomes small in the thick QWs so that their coupling by the off-diagonal terms of the Luttinger Hamiltonian omitted in our model becomes important. Heavy-hole-light-hole coupling redistributes oscillator strength between the heavy-hole and light-hole excitons. In the case of InGaAs/GaAs QWs, the strain-induced splitting of the heavy-hole and light-hole excitons suppresses their coupling, therefore our model is still applicable even for thick QWs.

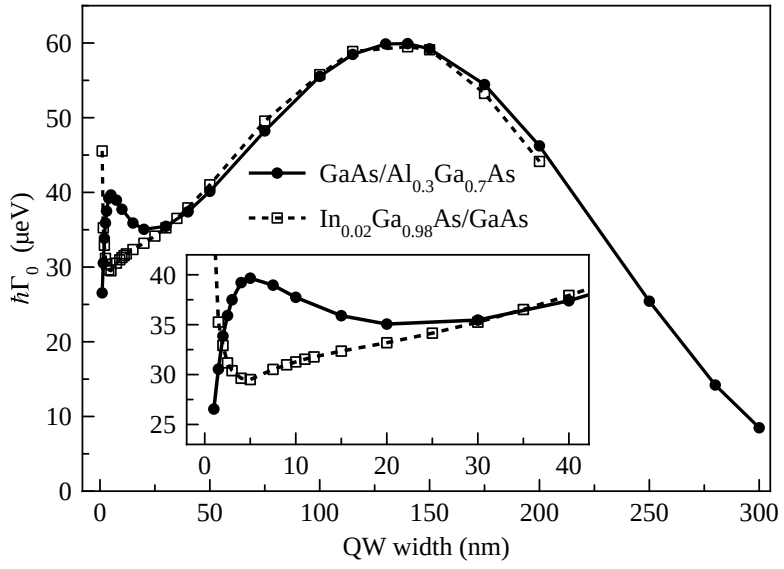

Figure 3. Radiative decay rate for GaAs/$Al_{0.3}Ga_{0.7}$As (solid curve) and $In_{0.02}Ga_{0.98}$As/GaAs (dashed curve) QWs of various widths from 1 nm to 300 nm and from 1 nm to 200 nm, respectively.

As the QW width decreases, Γ_0 also decreases due to the diminishing overlap integral in Eq. (6). For small QW widths, however, the behavior of Γ_0 for GaAs/$Al_{0.3}Ga_{0.7}$As and $In_{0.02}Ga_{0.98}$As/GaAs is different. For GaAs/AlGaAs one can see the growth of $\hbar\Gamma_0$ and a local maximum at $L \sim 5$ nm. This result is also confirmed by the experimental data in Ref. [15]. We may suppose that this maximum of Γ_0 is caused by squeezing of the exciton in the narrow QWs by the QW potential. The squeezing increases the probability to find the electron and the hole in the same position ($z_e = z_h$ and $\rho = 0$).

The opposite behavior is observed for $In_{0.02}Ga_{0.98}$As/GaAs as L decreases. One can see that $\hbar\Gamma_0$ diminishes as the QW width L decreases and there is no peak of $\hbar\Gamma_0$ at small QW widths.

We believe that this difference is related to different depths of the QWs. The absence of a peak is the indication of the weak exciton squeezing due to a small QW potential depth.

The rapid growth of $\hbar\Gamma_0$ at $L \to 0$ in the InGaAs/GaAs QWs can be explained by a stronger penetration of an exciton into the barriers as compared to the much deeper GaAs/AlGaAs QWs. Due to the penetration, the overlap of the exciton wave function $\Phi(z)$ and the light wave increases and, in turn, the radiative decay rate increases as $L \to 0$.

5. Conclusions

In summary, we have numerically obtained the radiative decay rate for the exciton ground state. For that, we have solved the three-dimensional equation, which was deduced from the electron-hole Hamiltonian with the Luttinger terms for the valence band. The direct microscopic solution using the fourth-order finite-difference scheme has been carried out for the first time. It allowed us to precisely calculate the exciton ground state energy and the exciton radiative decay rate. We obtained the radiative decay rates for GaAs/AlGaAs and InGaAs/GaAs heterostructures for various QW widths in the ranges of $1 \leq L \leq 300$ nm and $1 \leq L \leq 200$ nm, respectively.

Acknowledgments

Financial support from the Russian Ministry of Science and Education (contract no. 11.G34.31.0067), SPbU (grants No. 11.38.213.2014), RFBR and DFG in the frame of Project ICRC TRR 160 is acknowledged. The authors also thank the SPbU Resource Center "Computational Center of SPbU".

References

[1] Knox R 1963 *Theory of excitons* (New York: Academic press)
[2] Luttinger J M 1956 *Phys. Rev.* **102** 1030
[3] Baldereschi A and Lipari N C 1971 *Phys. Rev. B* **3** 439
[4] Andreani L C 1991 *Solid State Comm.* **77** 641
[5] Citrin D S 1993 *Phys. Rev. B* **47** 3832
[6] Andreani L C 1998 *Physica E* **2** 151
[7] Iotti R C and Andreani L C 1997 *Phys. Rev. B* **56** 3922
[8] D'Andrea A, Tomassini N, Ferrari L, Righini M, Selci S, Bruni M R, Schiumarini D and Simeone M G 1998 *J. Appl. Phys.* **83** 7920
[9] Deveaud B, Clérot F, Roy N, Satzke K, Sermage B and Katzer D S 1991 *Phys. Rev. Lett.* **67** 2355
[10] Zhang B, Kano S S, Shiraki Y and Ito R 1994 *Phys. Rev. B* **50** 7499
[11] Prineas J P, Ell C, Lee E S, Khitrova G, Gibbs H M and Koch S W 2000 *Phys. Rev. B* **61** 13863
[12] Deveaud B, Kappei L, Berney J, Morier-Genoud F, Portella-Oberli M T, Szczytko J and Piermarocchi C 2005 *Chem. Phys.* **318** 104
[13] Trifonov A V, Korotan S N, Kurdyubov A S, Gerlovin I Ya, Ignatiev I V, Efimov Yu P, Eliseev S A, Petrov V V, Dolgikh Yu K, Ovsyankin V V and Kavokin A V 2015 *Phys. Rev. B* **91** 115307
[14] Belykh V V and Kochiev M V 2015 *Phys. Rev. B* **92** 045307
[15] Poltavtsev S V and Stroganov B V 2010 *Phys. Solid State* **52**, 1899 [*Fiz. Tverd. Tela* **52** 1769].
[16] Poltavtsev S V, Efimov Yu P, Dolgikh Yu K, Eliseev S A, Petrov V V and Ovsyankin V V 2014 *Solid State Comm.* **199** 47
[17] Loginov D K, Trifonov A V and Ignatiev I V 2014 *Phys. Rev. B* **90** 075306
[18] Bastard G, Mendez E E, Chang L L and Esaki L 1982 *Phys. Rev. B* **26** 1974
[19] Samarskii A A 1989 *The theory of difference schemes* (Moscow: Nauka)
[20] Sorensen D C, Lehoucq R B and Vu P 1995 *ARPACK: an implementation of the Implicitly Restarted Arnoldi iteration that computes some of the eigenvalues and eigenvectors of a large sparse matrix*
[21] Gerlach B, Wüsthoff J, Dzero M O and Smondyrev M A 1998 *Phys. Rev. B* **58** 10568
[22] Vurgaftman I, Meyer J R and Ram-Mohan L R 2001 *J. Appl. Phys.* **89** 5815
[23] Glinskii G F, Lakisov V A, Dolmatov A G and Kravchenko K O 2000 *Nanotechnology* **11** 233
[24] Ivchenko E L 2005 *Optical spectroscopy of semiconductor nanostructures* (Harrow: Alpha Science Int.)